Influence of Axial Temperature Profiles on Fe/SiO_2 Catalyzed Non-oxidative Coupling of Methane

Rolf S. Postma[a] and Leon Lefferts*[a]

The effect of the axial temperature profile upstream and downstream of catalyst bed on the performance of non-oxidative-coupling-of-methane (NOCM) over Fe/SiO_2 was determined. A three-zone oven was used with independent temperature control of the catalyst-zone as well as the zones upstream and downstream. It was found that catalytic initiation followed by residence time at 1000 °C downstream the catalyst bed increases CH_4 conversion by a factor of 8, while decreasing carbonaceous deposit selectivity from 40 to 12 C%. Residence time at 1000 °C upstream of the catalyst bed causes deposit formation on the catalyst without significantly influencing methane conversion. A shallow catalyst bed followed by significant residence time at high temperature maximizes methane conversion and minimizes coking. This work shows that axial temperature profile and residence time upstream and downstream of the catalyst bed strongly influence the performance in catalytic NOCM.

Methane[1] is one of the most abundant hydrocarbons on the planet[2] and is seen as a high potential intermediate in the transition towards renewable sources of chemicals.[3] Currently, methane is mainly used in domestic and industrial heating as well as electricity production.[4] The vast majority of industrial processes for converting natural gas into base chemicals and liquid fuels is based on reforming[5] followed by various syngas-based synthesis routes.[5a,b,6] The multiple steps in these processes cause low energy efficiency and high investment costs.[6c,7]

Thus, direct methane coupling has received a lot of attention both in industry as well as academia.[3,8] The challenge is caused by the high stability of methane, its negligible electron affinity and low polarizability,[9] compared to the coupling products. Both Methane dehydroaromatization (MDA)[5c,8a,b,d,f] as well as oxidative coupling of methane (OCM)[5c,8c,10] suffer from too low product yields to be industrially viable. Catalytic NOCM[2b,11] has recently gained much interest, achieving higher product yield and co-producing valuable hydrogen. The NOCM reaction requires operation temperatures above 900 °C, to achieve significant conversion[9a] usually resulting in significant coke formation.

In 2014 Guo et al.[2b] reported coupling of methane to olefins and aromatics over an iron on silica catalyst (Fe/SiO_2) at temperatures in excess of 950 °C, without coke formation. The maximum reported combined product yield was 48% at 1090 °C. Other research groups also report low coking rates but have not yet been able to reproduce the performance reported by Guo *et al.*.[11a–c,i,12] An overview of literature data on catalytic non-oxidative methane coupling is presented in S1. Despite the fact that many laboratories initiated work on the subject, the number of peer reviewed papers is rather limited, likely because it is not easy to prevent extensive coking. We will show in this study that the design of the lab reactor and the oven is essential for achieving this.

Methane is thermodynamically unstable at temperatures above 650 °C,[9a,13] which is confirmed by the blank experiments in several studies,[2b,11b,c] showing significant methane conversion. DFT calculations[2b,11i] suggest that the Fe/SiO_2 catalyst is involved exclusively in methane activation to methyl radicals and hydrogen, which are released to the gas phase. All further coupling reactions to olefins and aromatics are governed by gas phase free-radical propagation and termination reactions.[2b,11i] Especially the recent patent[12] issued by Sabic supports this, showing that reactions in the gas phase downstream the catalyst bed influence conversion and product distribution significantly. It is remarkable that detailed information on reactor design, oven design, dimensions and temperature profile around the catalyst bed are generally not available.[2b,11a–d, f,h,12] This study demonstrates that axial temperature profiles, controlled with an oven designed for this purpose, influence not only conversion and product distribution, but also the formation of carbonaceous deposits significantly.

A custom-built oven was used to control the temperature profile in the reactor-zone, as well as the zones upstream and downstream of the catalyst bed (Figure 1). The temperature in each of the three zones is controlled independently up to 1100 °C. Sharp temperature gradients were achieved by using close fitting thermal insulation between the zones. Residence time at high temperature upstream, inside and downstream of the catalyst bed were systematically changed by varying the amount of catalyst, the position of the catalyst bed inside the

[a] R. S. Postma, Prof. L. Lefferts
Catalytic Processes and Materials group
Faculty of Science and Technology
MESA + Institute for Nanotechnology
University of Twente
PO Box 217
Enschede, 7500 AE (Netherlands)
E-mail: l.lefferts@utwente.nl

Supporting information for this article is available on the WWW under https://doi.org/10.1002/cctc.202001785

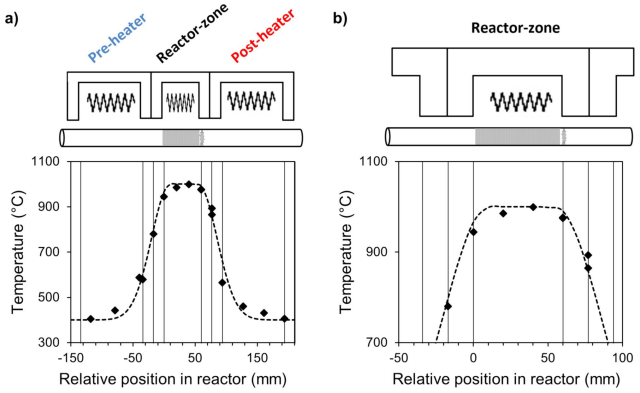

Figure 1. a) Temperature profile inside the reactor measured with an empty reactor tube b) zoom in on Figure 1a; gas-flow rates of 10 ml/min N_2; Vertical bars represent the insulating layers between the 3 different zones. Pre- and post-heater at 400 °C; reactor-zone at 1000 °C.

6 cm reactor-zone as well as the temperatures of the pre-heater and the post-heater.

The terms "τ@upHT" and "τ@downHT" refer respectively to residence time at 1000 °C upstream of downstream of the catalyst bed. All residence times are calculated based on the volume of the relevant part of the reactor and the flowrate at STP. Details concerning the experimental setup and the equations applied to calculate conversion and selectivity to several products can be found in S4 and S5, respectively.

Figure 2 shows increasing methane conversion with increasing residence time at 1000 °C downstream of the catalyst bed (τ@downHT), at constant conditions and contact time inside the catalyst bed. This effect is not observed when increasing residence time at 1000 °C upstream of the catalyst bed (τ@upHT), as shown in Figure S6. The conversion under the same conditions in absence of catalyst is low (Figure 2), in agreement with the hypothesis that the catalyst activates methane, forming methyl radicals,[2b,11i] followed by radical chain reactions. A similar autocatalytic phenomenon is also reported for non-catalytic non-oxidative coupling of methane.[13c,14] Apparently, residence time at high temperature downstream of the catalyst bed enables propagation of the radical chain reaction, increasing methane conversion substantially. Remarkably, this effect continues for at least 8 seconds residence time.

Figure 3 shows the effect of τ@downHT on the yields of products. The yields of all products increase in the hot volume downstream the catalyst bed as conversion increases, except for the yield of ethane. Apparently, increasing consecutive conversion of ethane in the hot zone dominates over formation of ethane. Yield of carbon deposits, estimated assuming a closing C-mass balance, increases much less with increasing methane conversion than the other products (Figure 3a). Figure S7 presents the trends in selectivity with τ@downHT at constant conversion, confirming that the selectivity to carbon deposits decreases. In contrast, yields of acetylene, benzene

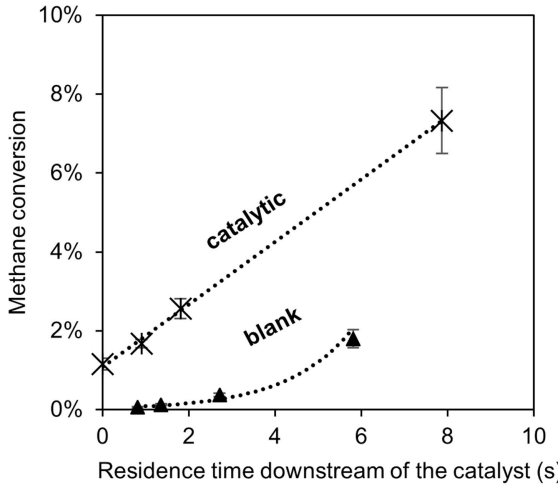

Figure 2. The effect of post-catalytic free-volume residence time at 1000 °C, ✱ for methane activated by 0.26 g catalyst at 3.5 l g_{cat}^{-1} h^{-1}, ▲ gas-phase initiated system (no catalyst); 90 % CH_4 in N_2; reactor-zone at 1000 °C, pre-heater at 400 °C; post-heater at 400 °C for lower residence time in free volume and 1000 °C for higher residence time in free volume

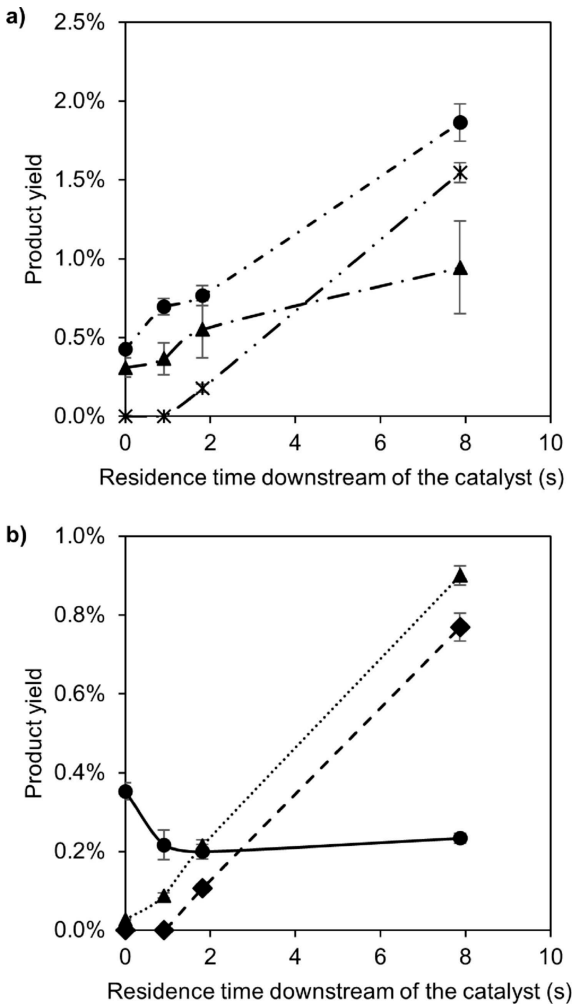

Figure 3. Influence of τ@downHT on the yield at 3.5 l g_{cat}^{-1} h^{-1}; 0.26 g catalyst; 90 % CH_4 in N_2; (a) major products: — ✱ — Naphthalene; - ·●· - Ethylene; —▲— Deposits; (b) minor products: —●— Ethane; – ◆ – Benzene; ·····▲····· Acetylene; conditions according to Figure 2.

Table 1. Performance comparison between this work and others using the Fe/SiO_2 catalyst.

Publication	Conditions/ref	Temp [°C]	SV [ml g_{cat}^{-1} h^{-1}]	Conversion [%] CH_4	Olefins selectivity [C%]	Aromatics selectivity [C%]	Deposit selectivity [C%]
This work	Fast quenching	1000	3650	0.9	61	0	39
This work	τ@downHT 8 sec	1000	3640	7.7	50	38	12
Guo et al.	[2b]	1000	10000	31	21	79	0
Sakbodin et al.	[11a]	1000	3200	8%	37	63	0
Oh et al.	[11b]	1000	3200	8%	37	53	10
Han et al.	[11c]	1020	8250	6.5%	66	32	2
Nagaki et al.	[12]	1030	21400	7.5	44	50	6

and naphthalene all significantly increase and their production via free radical chain reactions apparently dominates over consecutive conversion reactions in the hot zone downstream the catalyst.

Table 1 compares the performance of Fe/SiO_2 in this work, both with and without extended residence time at 1000 °C downstream of the catalyst bed, with the results reported in literature. It is remarkable that both activity as well as selectivity obtained when operating with high τ@downHT, are quite similar to results of Sakbodin et al. and Oh et al. .[11a,b] In contrast, fast quenching downstream of the catalyst bed results in much lower conversion and more deposit formation.

Figure 4 shows that the apparent activation energy increases with increasing τ@downHT, based on experiments between 950 and 1100 °C. We observe that apparent activation energy increases with increasing methane conversion in τ@downHT. Han *et al.*[11c] reported an apparent activation energy of 334 kJ mol^{-1}. Calculation of apparent activation energies based on the data of Guo *et al.*,[2b] Sakbodin *et al.*[11a] and Oh et al.[11b] resulted in 454 kJ mol^{-1}, 333 kJ mol^{-1} and 577 kJ mol^{-1} respectively, as presented in Figure S12. A coated wall reactor contains a large empty volume, explaining the high activation energy estimated based on the data of Oh. The high activation barrier estimated based on the results of Guo suggests a large contribution of reactions in the downstream zone, in agreement with the fact that conversion and activity were the highest reported so far. To lesser extent, the same is true for the results reported by Sakbodin et al.[11a] and Han et al..[11c]

Figure 5 presents the integral yields to products, deposits on the catalyst and deposits downstream during a 14 hours experiment under conditions as summarized in Table S3. Figure 5 confirms that the product yield increases with increasing τ@downHT. Figure 5 also shows that formation of deposits on the catalyst is suppressed by rapid heating of the reactant gas before it reaches the catalyst, preventing soot formation in the gas phase that would be trapped by the catalyst bed.

In summary, methane conversion is dominated by propagation reactions in free volume at 1000 °C downstream of the

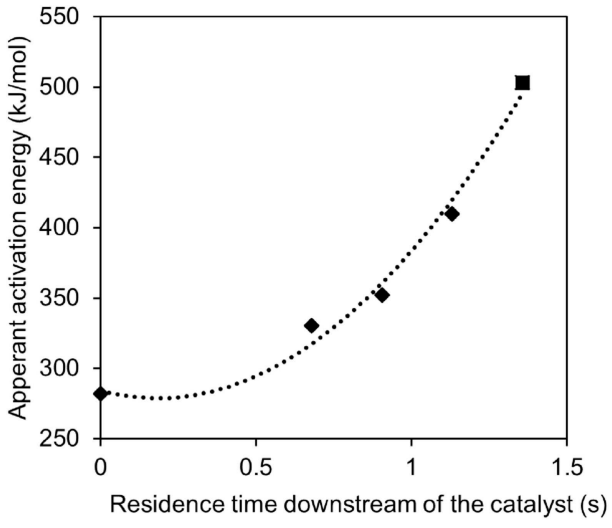

Figure 4. Apparent activation energy change when increasing the free-volume downstream of the catalyst, by decreasing the amount of catalyst; measured at constant flowrate: 33.3 ml/min: 90% CH_4 in N_2 ◆; temperature of reactor-zone varied between 950–1100 °C, pre-heater and post-heater at 400 °C; note that the data point ■ at 1.35 S has **no** catalyst; for details on catalyst placement see S4 in the Supporting Information.

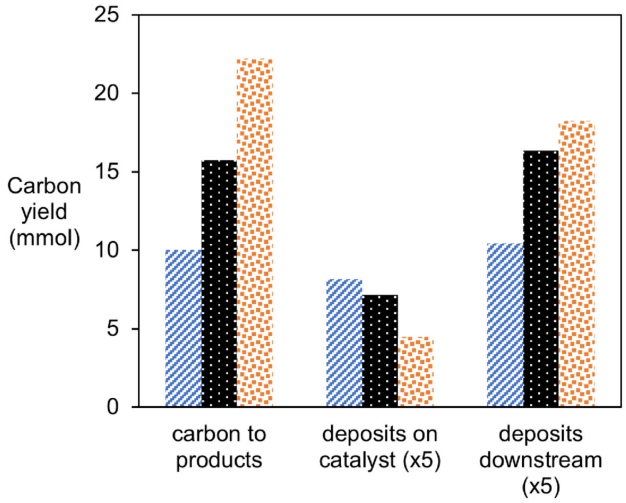

Figure 5. Effect of τ@upHT and τ@downHT on the integral product distribution over a full experiment during 14 h at 1000 °C with 90% CH_4 in N_2 during which flowrate and temperature was varied in time according a fixed program described in Table S3; ▨ 0.5 ml τ@upHT; ■ 0.25 ml τ@upHT & 0.25 ml τ@downHT; ▩ 0.5 ml τ@downHT; deposits on the catalyst are measured using TGA and assumed to contain exclusively carbon. Deposit formation downstream of the catalyst estimated based on the C-mass balance; deposits on the catalyst and downstream of the catalyst have been multiplied by 5 for clarity; pre-heater and post-heater operated at 400 °C.

catalyst bed, after initiation of the free radical reaction by the catalyst, in agreement with the recent patent publication.[12] At the same time, formation of deposits is significantly reduced, whereas formation of olefins and aromatics in the hot zone dominate. Formation of deposits can be further suppressed by heating the reaction mixture rapidly, before contacting the catalyst. Residence time inside the catalyst bed should be minimized, since the catalyst is only required for initiation the free radical reaction and will cause significant deposit formation when in contact with free radicals.

The design of the catalytic reactor and the oven determines to an important extent the performance in catalytic NOCM, with respect to both activity as well as minimizing formation of deposits. Unfortunately, these details are usually not reported. Especially the large effect on the formation of carbonaceous deposits is responsible for the fact that results depend strongly on experimental details.

Experimental section

The Fe/SiO_2 catalyst was prepared according procedures reported in literature[2b] and the expected composition and structure were confirmed with XRF and XRD, respectively.[2b,11a, c] More detailed information on catalyst synthesis and characterization is presented in S2 and S3, illustrating our catalyst is very similar to Fe/SiO_2 catalysts synthesized in earlier studies.

Acknowledgements

We acknowledge support from the Dutch National Science Foundation (NWO) and the industrial partners: Sabic, Sasol and BASF. We thank ing. B. Geerdink, K.J. Altena, ing. T.L.M. Velthuizen and ir. T. Lubbers for their experimental and analytical support. We thank dr. A. Nijhuis and dr. D. Nagaki for inspiring discussions. Lastly, we thank dr. E. Postma for input in correcting the document.

Conflict of Interest

The authors declare no conflict of interest.

Keywords: Fe©SiO_2 · non-oxidative methane conversion · free radical reaction · coke formation

[1] a) M. M. Foss, Center for Energy Economics, **2004**; b) Uniongas, *Chemical Composition of Natural Gas* **2017**.
[2] a) BP plc, *BP Statistical Review of World Energy 2019* **2019**; b) X. Guo, G. Fang, G. Li, H. Ma, H. Fan, L. Yu, C. Ma, X. Wu, D. Deng, M. Wei, D. Tan, R. Si, S. Zhang, J. Li, L. Sun, Z. Tang, X. Pan, X. Bao, *Science* **2014**, *344*, 616–619.
[3] P. Schwach, X. Pan, X. Bao, *Chem. Rev.* **2017**, *117*, 8497–8520.
[4] U. S. Energy information administration, International Energy Outlook 2016; Chapter 3: natural gas **2016**.
[5] a) A. d. Klerk, in *Kirk-Othmer Encycl. Chem. Technol.* **2013**, pp. 1–20; b) H. A. Wittcoff, B. G. Reuben, J. S. Plotkin, *John Wiley & Sons, Inc.* **2012**; c) R. J. Kee, C. Karakaya, H. Zhu, *Proc. Combust. Inst.* **2017**, *36*, 51–76.
[6] a) B. Wang, S. Albarracín-Suazo, Y. Pagán-Torres, E. Nikolla, *Catal. Today* **2017**, *285*, 147–158; b) K. Huang, J. B. Miller, G. W. Huber, J. A. Dumesic, C. T. Maravelias, *Joule* **2018**, *2*, 349–365; c) I. Amghizar, L. A. Vandewalle, K. M. V. Geem, G. B. Marin, *Engineering* **2017**, *3*, 171–178.
[7] S. Mohajerani, A. Kumar, A. O. Oni, *Energy* **2018**, *150*, 681–693.
[8] a) A. Galadima, O. Muraza, *Catal. Surv. Asia, 23*, 149–170; b) K. Sun, D. M. Ginosar, T. He, Y. Zhang, M. Fan, R. Chen, *Ind. Eng. Chem. Res.* **2018**, *57*, 178–1789; c) W. Taifan, J. Baltrusaitis, *Appl. Catal. B* **2016**, *198*, 525–547; d) A. I. Olivos-Suarez, A. G. Szécsényi, E. J. M. Hensen, J. Ruiz-Martinez, E. A. Pidko, J. Gascon, *ACS Catal.* **2016**, *6*, 2965–2981; e) C. Mesters, *Annu. Rev. Chem. Biomol. Eng.* **2016**, *7*, 223–238; f) E. V. Kondratenko, T. Peppel, D. Seeburg, V. A. Kondratenko, N. Kalevaru, A. Martin, S. Wohlrab, *Catal. Sci. Technol.* **2017**, *7*, 366–381; g) C. Karakaya, R. J. Kee, *Prog. Energy Combust. Sci.* **2016**, *55*, 60–97.
[9] a) C. Guéret, M. Daroux, F. Billaud, *Chem. Eng. Sci.* **1997**, *52*, 815–827; b) F. A. Carey, R. J. Sundberg, in *Advanced Organic Chemistry Part A: Structure and Mechanisms*, Springer, **2007**.
[10] a) B. L. Farrell, V. O. Igenegbai, S. Linic, *ACS Catal.* **2016**, *6*, 4340–4346; b) Y. Gao, L. M. Neal, D. Ding, W. Wu, C. Baroi, A. Gaffney, F. Li, *ACS Catal.* **2019**.
[11] a) M. Sakbodin, Y. Wu, S. C. Oh, E. D. Wachsman, D. Liu, *Angew. Chem.* **2016**, *55*, 16149–16152; b) S. C. Oh, E. Schulman, J. Zhang, J. Fan, Y. Pan, J. Meng, D. Liu, *Angew. Chem.* **2019**, *58*, 7083–7086; c) S. J. Han, S. W. Lee, H. W. Kim, S. K. Kim, Y. T. Kim, *ACS Catal.* **2019**, *9*, 7984–7997; d) Y. Chen, X. Wang, X. Luo, X. Lin, Y. Zhang, *Chin. J. Chem.* **2018**, *36*, 531–537; e) C. Okolie, Y. Lyu, L. Kovarik, E. Stavitski, C. Sievers, *ChemCatChem* **2018**, *10*, 2700–2708; f) P. Xie, T. Pu, A. Nie, S. Hwang, S. C. Purdy, W. Yu, D. Su, J. T. Miller, C. Wang, *ACS Catal.* **2018**, *8*, 4044–4048; g) Y. Xiao, A. Varma, *ACS Catal.* **2018**, *8*, 2735–2740; h) Y. Nishikawa, H. Ogihara, I. Yamanaka, *ChemistrySelect* **2017**, *2*, 4572–4576; i) S. K. Kim, H. W. Kim, S. J. Han, S. W. Lee, J. Shin, Y. T. Kim, *Commun. Chem.* **2020**, *3*, 1–8.
[12] D. A. Nagaki, Z. Zhao, M. N. Z. Myint, I. Lengyel, A. Mamedov, C. W. Gundlach, K. Sankaranarayanan, D. Falcone, in *USPatent Office*, Sabic Global Technologies, B. V., United States of America, **2018**.
[13] a) G. P. v. d. Zwet, P. A. J. M. Hendriks, R. A. v. Santen, *Catal. Today* **1989**, *4*, 365–369; b) W. E. Slater, *J. Chem. Soc. Trans.* **1916**, *109*, 160–164; c) A. M. Dean, *J. Phys. Chem.* **1990**, *94*, 1432–1439; d) C. J. Chen, M. H. Back, *Can. J. Chem.* **1975**, *53*, 3580–3590.
[14] J. M. Roscoe, M. J. Thompson, *Int. J. Chem. Kinet.* **1985**, *17*, 967–990.

Manuscript received: November 3, 2020
Revised manuscript received: November 29, 2020
Accepted manuscript online: November 30, 2020
Version of record online: ■■, ■■■

COMMUNICATIONS

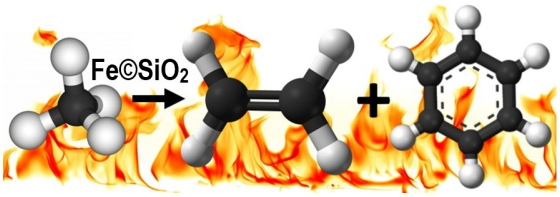

*R. S. Postma, Prof. L. Lefferts**

Higher methane conversion, lower coking: The axial temperature profile in a catalytic reactor for non-oxidative methane pyrolysis over Fe/SiO_2 strongly influences the performance. Extended residence time at 1000 °C downstream of the catalyst significantly increases methane conversion and decreases formation of carbonaceous deposits, while decreasing residence time at 1000 °C upstream of the catalyst bed also suppresses formation of deposits.